Detachment of Oil Drops from Solid Surfaces in Surfactant Solutions: Molecular Mechanisms at a Moving Contact Line†

Peter A. Kralchevsky,*,‡ Krassimir D. Danov,‡ Vesselin L. Kolev,‡ Theodor D. Gurkov,‡ Mila I. Temelska,‡ and Günter Brenn§

Laboratory of Chemical Physics & Engineering, Faculty of Chemistry, University of Sofia, 1164 Sofia, Bulgaria, and Institute of Fluid Mechanics and Heat Transfer, Graz University of Technology, 8010 Graz, Austria

Here, we present experimental data and a theoretical model for the dynamics of detachment of hexadecane drops from a solid substrate (glass plate) in aqueous solutions of anionic surfactant and salt, at various temperatures. The influence of the experimental conditions on the motion of the three-phase contact line is investigated. We found indications that water molecules can propagate by lateral diffusion in a thin layer on the surface of the solid plate. The driving force of the detachment process, viz., the imbalance of the interfacial tensions at the contact line, is engendered by the water penetration, while the line friction force compensates this imbalance and determines the stationary speed. Excellent agreement between theory and experiment is achieved. The present study specifies the parameters that can be used to quantitatively characterize the rate of drop detachment, determines the values of these parameters at various experimental conditions, and indicates tools for control of the investigated spontaneous process.

1. Introduction

Processes with a moving contact line are crucial for many applications in coating, printing, painting, detergency, and membrane emulsification. The most studied are the cases when the motion of the contact line on a solid surface is strained by some external force or potential gradient, including processes of liquid deposition on a moving or porous substrate; see refs 1−14 and the literature cited therein. In contrast, in the case of a *diffusional* mechanism, observed for oily drops detaching from a solid surface in water,[15,16] the contact-line motion occurs spontaneously, at a nonzero contact angle, driven by some molecular mechanisms; for example, water and surfactant diffuses between the oil and solid. The velocity of the latter process is much lower than that in the case of conventional spreading (zero contact angle; see, e.g., ref 17) or superspreading.[18]

Several mechanisms have been discussed in the literature in relation to the cleaning of solid surfaces from oily deposits. The most popular of them are the roll-up, emulsification, and solubilization.[19−26] Depending on the specific system, one or another mechanism can prevail. From a practical viewpoint, it is important to reveal the physicochemical factors that can be used for efficient control of the cleaning process, some of them being the type and concentration of the used surfactants and electrolytes.[15,16,27−31] Technologically oriented experiments on the detachment of oil drops from solid substrates were carried out by Dillan et al.,[21] who obtained much data about the efficiency of the roll-up mechanism. The experiments indicate that the apparent "roll-up" is related to a shrinking of the three-phase contact line solid−oil−water, which, in its own turn, is due to the molecular penetration (diffusion) of water molecules between the oil drop and the solid phase.[15] The latter process was termed the diffusional mechanism of oil detachment. Chatterjee investigated the critical conditions for buoyancy-induced detachment of oil drops from a substrate due to instability in the shape of the oil−water interface.[32,33]

Wasan et al.[15] investigated the detachment of crude-oil drops from glass in solutions of 1 wt % C_{16}-α-olefin sulfonate + 1 wt % NaCl. These authors observed directly the dynamics of water-film penetration between the oil phase and the solid. Once such a disjoining aqueous film has been formed, even a weak shear flow is able to detach the oil drop from the substrate. The study in ref 15 is related to the enhanced oil recovery; however, a similar mechanism can be operative also for oil-drop detachment in other applications of detergency.

Our previous study[16] was directed toward analyzing the mechanism of spontaneous detachment of oil drops from solid surfaces in solutions of ionic surfactants. We carried out direct microscopic observations of the cleaning process for a hydrophilic glass surface, in an attempt to reveal the main stages of the oil-drop detachment. Our attention was focused on the balance of forces at the moving three-phase contact line. In such cases, a line friction force has to be included in the Neumann−Young force balance at the contact line.[34,35] Analyzing the experimental data, we found that this friction force is proportional to the velocity of contact-line motion. From the slope of the respective linear regression, the line friction coefficient was determined for the specific system investigated.[16]

The physical origin of the line friction force, and its importance for various processes with dynamic contact lines, was discussed in a number of studies by Blake et al.,[10,35] de Coninck et al.,[36−41] Attard,[34] and von Bahr et al.[42] In our experiments,[16] we found that the relaxation of the contact angle toward its equilibrium value is impeded and decelerated by the line friction force.

† This paper is dedicated to Professor Darsh T. Wasan on the occasion of his 65th birthday.

* To whom correspondence should be addressed. Tel.: (+359) 2-962 5310. Fax: (+359) 2-962 54 38. E-mail: pk@lcpe.uni-sofia.bg.

‡ University of Sofia.

§ Graz University of Technology.

10.1021/ie049211t CCC: $30.25
Published on Web 12/24/2004

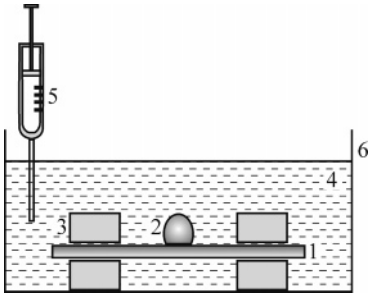

Figure 1. Scheme of the experimental cell: 1, glass plate; 2, oil droplet $\approx 1\ \mu$L; 3, glass holders; 4, surfactant solution; 5, syringe; 6, cuvette.

Thus, it turns out that the magnitude of the line friction coefficient, β, determines the rate of shrinking of the contact line and, consequently, the overall time of oil-drop detachment. (In a similar way, the bulk viscosity of a liquid determines the velocity of a falling heavy ball.) Hence, the value of β, and its dependence on the experimental conditions, represents a problem of scientific and practical importance that deserves a more detailed investigation.

The present paper is a continuation of our previous study[16] in two aspects. First, we examine systematically the effect of the most important factors (temperature and surfactant and salt concentrations) on the dynamics of drop detachment. Second, we develop a quantitative theoretical model, which enables us to fit the experimental dependence of the contact-line radius on time and to determine the values of the involved physicochemical parameters.

The paper is organized as follows. In section 2, we describe the experimental system and method. The experimental results are presented and discussed in section 3. The theoretical model is described in section 4. Finally, section 5 is devoted to the comparison of theory and experiment and to data interpretation. The results reveal that the penetration and diffusion of water in a thin layer on the solid surface could be rather important for the dynamics of oil-drop detachment.

2. Experimental Section

In our experiments, the oil phase was pure hexadecane (Aldrich). The water phase was an anionic surfactant solution. We used two surfactants, sodium dodecyl sulfate (SDS, a product of Merck), and C_{16}-α-olefin sulfonate (AOS, the technical product Hostapur OSB of Clariant). As an inorganic electrolyte, we used pure NaCl. In the experiments, we investigated the role of three factors: (i) surfactant concentration, (ii) NaCl concentration, and (iii) temperature.

We applied a simple experimental setup, which is sketched in Figure 1. A square glass plate, 22×22 mm, representing a plane-parallel microscope slide (manufactured by Menzel-Glaser), serves as a substrate. To avoid irreproducible variations in the surface properties of the glass, in each experiment a new slide was used as received directly from the manufacturer, without any previous treatment. The slide was positioned horizontally on two rectangular glass holders in a cuvette. The slide was pressed down by two other glass pieces (3 in Figure 1).

Initially, on the *dry* glass plate, we place a hexadecane drop (of volume $\approx 1\ \mu$L) by means of a microsyringe. This drop is left to stay for about 10 min, to achieve stronger adhesion to the substrate. Then, we add a surfactant solution of volume 20 mL. It is loaded in a syringe (5 in Figure 1) and flows slowly through its needle to cover the drop as gently as possible. It is important to adjust the horizontal level of the glass slide so that the liquid is wetting it uniformly in all directions. Often, a part of the drop detaches immediately after its contact with the surfactant solution (necking instability due to the buoyancy force), but a residual (smaller) oil drop remains on the substrate. Further, we observe and record the evolution of this residual drop; see the illustrative photographs in Figure 2. In all experiments, with elapsed time, the contact line shrinks, the oil−solid contact area decreases, and the drop becomes vertically elongated under the action of buoyancy (pendant-drop-type profile). At the final stage (Figure 2, last photograph), a neck is formed. Next, the drop detaches very quickly. Usually, the drop detaches completely, without formation of a new residual drop.

The observation of the drop profile was performed from the side, through the wall of the glass cuvette. A horizontal microscope, equipped with an objective of long focal distance, was applied for this purpose. A digital CCD camera (Kappa CF 8/1 DX) and VCR (Samsung SV-4000) were used to record the pictures. For most systems, we performed three independent runs monitoring the time evolution of the shape of three drops with different sizes, from the moment of addition of the aqueous solution until the eventual drop detachment. This process takes place at a fixed volume of the drop. In other words, the solubilization of oil by the micelles in the investigated surfactant solutions is negligible. This was checked by experiments with single drops, applying the method described in ref 43.

Images of the drop shape were continuously taken by the CCD camera and recorded. Pictures, corresponding to consecutive moments (like those in Figure 2), were digitized, assigning coordinates to a number of points on the drop profile. An example is given in Figure 3. Then, the experimental points are fitted with the Laplace equation of capillarity. The best fit is shown by the continuous line in Figure 3. Details about the processing of the drop profiles are given in section 3 of ref 16. From the Laplace fits, we obtained the values of the contact-line radius, r_c, contact angle, α (see Figure 3), and the oil−water interfacial tension, σ, as functions of time, t. In fact, the determination of σ from the drop profile is analogous to the known pendant drop method or to the axisymmetric drop shape analysis; see, e.g., ref 44.

It should be noted that the occurrence of the drop detachment depends strongly on the state of the glass surface. In control experiments, we kept the glass plates immersed in pure water for 1 h (instead of using them dry, without any pretreatment). After that, the plates were dried for 5 min in a vacuum drier and used in the experiments. Instead of the slow process in Figure 2, we observed that the hexadecane drops detach immediately from such glass substrates. The latter behavior can be attributed to the penetration of water molecules in a thin layer ("gel layer") on the surface of these glass plates, which have been preimmersed in water.[16]

3. Experimental Results and Discussion

3.1. Effects of the Surfactant, Electrolyte, and Temperature. Figures 4−7 show experimental data for

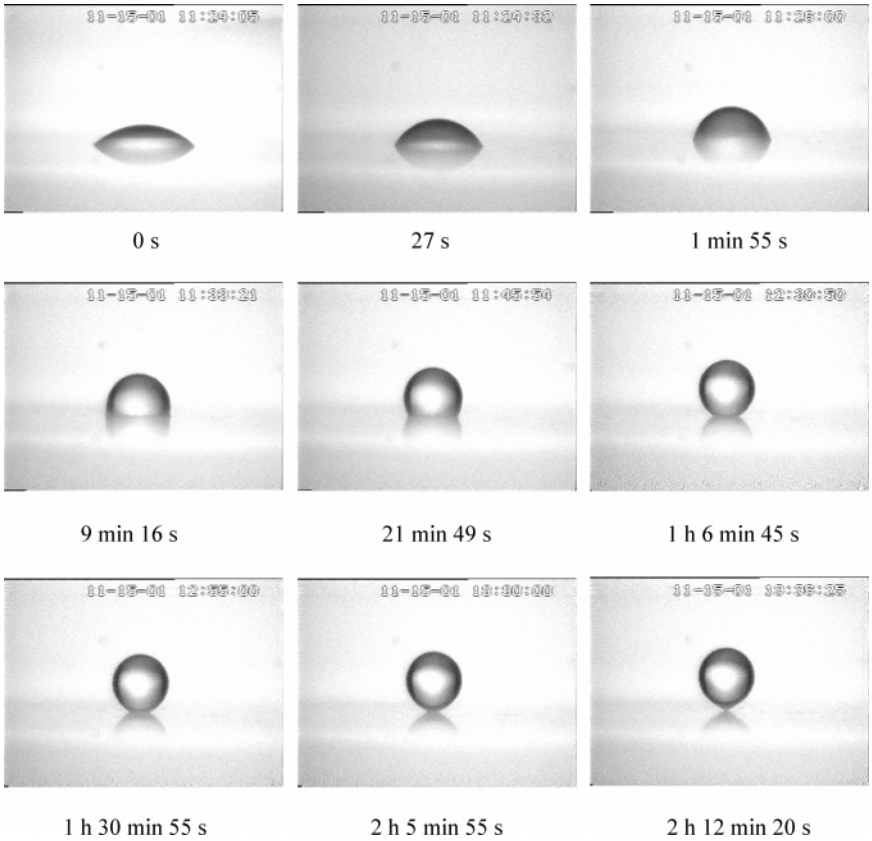

Figure 2. Consecutive photographs of the spontaneous detachment of a hexadecane drop from a horizontal glass plate immersed in a solution of 20 mM SDS + 0.1 mM NaCl at 23 °C. The drop volume is constant, 0.7415 mm^3.

the time dependence of the contact-line radius, r_c, and angle, α, for hexadecane drops (like that in Figure 2). In each figure, the data for r_c and α, denoted with identical symbols, correspond to the same drop. Every experimental point is obtained from a digitized drop profile, like those in Figure 3. In Figures 4a−7a, the symbols denote the experimental r_c while the solid lines connect the respective theoretical values of r_c, obtained by fitting the data with the help of the model described in section 4. A discussion about the comparison of theory and experiment is given in section 5.2.

Figures 4−7 show that initially r_c and α decrease quickly, but later their variation slows down. Most probably, such behavior is caused by a decreasing (relaxing) imbalance of the interfacial tensions at the three-phase contact line (see eq 3.2). At the final stage of the process, the contact-line radius r_c becomes so small that a neck begins to form; see Figures 2 and 3b. In Figures 4b−7b, the necking is manifested as an increase of α at the last stage of drop evolution, just before the drop detachment from the substrate. The contact angle, α, varies (decreases and increases) during the whole process, without reaching any equilibrium value, α_{eq}. In this respect, the present data differ from our previous experimental results,[16] where α leveled off at a constant value, which could be interpreted as the equilibrium value of α. We believe that the difference is due to the different types of glass plates used in the two experiments as substrates. On the other hand, the shapes of the obtained $r_c(t)$ dependencies are similar in the two experiments (here and in ref 16).

Figure 4 shows data for four hexadecane drops at four different surfactant (SDS) concentrations. Figure 5 shows similar data but for different concentrations of AOS. In general, one sees that the time needed for drop detachment decreases with the rise of the surfactant concentration. Figure 6 demonstrates that the electrolyte concentration has a strong effect on the drop detachment time: the latter significantly decreases with the rise of the NaCl concentration. Finally, Figure 7 indicates an analogous effect of the temperature: the drop detachment is faster at higher temperatures.

Note, however, that the detachment time depends not only on physicochemical factors, such as the temperature and surfactant and salt concentrations, but also on a geometrical factor: the drop volume (longer detachment for bigger drops). For this reason, the detachment time is not an appropriate physical characteristic of the process dynamics. As mentioned above, it is difficult to carry out experiments with drops of identical volume. (After the surfactant solution is poured, some part of the oil drop spontaneously detaches because of necking instability, and we perform the experiment with the residual drop whose volume is different in different runs.) Therefore, it is better to characterize the dynamics of drop detachment with parameters that are independent of the drop volume. The theoretical analysis of the above experimental data indicates that the *penetration time*, t_p, and the *line friction coefficient*, β, are independent of the drop volume and are adequate dynamic characteristics of the investigated process (see below).

3.2. Discussion of the Experimental Dependencies. Coming back to the experimental results, we should note that all values of the contact angle α in Figures 4−7 are dynamic (nonequilibrium). At fixed drop volume, V, the value of the contact-line radius, r_c, unequivocally determines the value of the contact angle, α. Indeed, purely geometrical considerations give the dependence $V = V(r_c,\alpha)$, which can be represented also

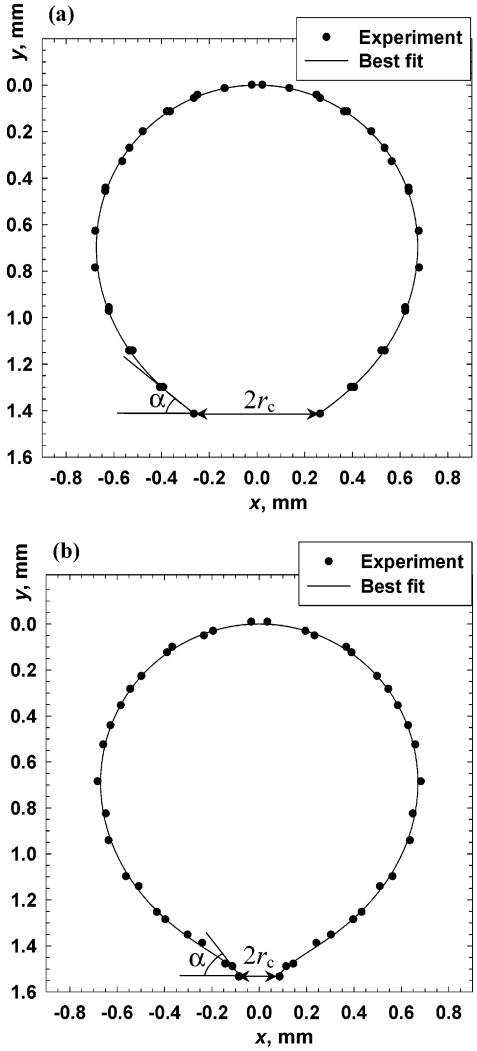

Figure 3. Digitized profiles of two photographs of the same drop, taken at different moments. The hexadecane drop has a volume of 1.377 mm^3 and is placed in a solution of 20 mM SDS + 0.1 mM NaCl. The theoretical line is drawn by fitting of the experimental points by means of the Laplace equation.[16] From the fit, we determine the contact-line radius, r_c, the contact angle, α, and the oil−water interfacial tension, σ.

in the form $\alpha = \alpha(V,r_c)$. The latter dependence can be easily derived for a spherical oil−water interface (see, e.g., eq 4 in ref 37), but an analogous dependence exists also for a drop profile that is deformed by gravity ("pendant drop" profile); the latter can be computed numerically by integration of the Laplace equation.[16] In other words, the measured dynamic contact angle, α, is a purely geometrical characteristic (determined by the position, r_c, of the shrinking contact line), in contrast with the *equilibrium* contact angle, α_{eq}, which is a physical parameter, related to the interfacial tensions through the Young equation

$$\sigma_{os} = \sigma_{ws} + \sigma_{eq} \cos \alpha_{eq} \tag{3.1}$$

where σ_{os} and σ_{ws} are the interfacial tensions of the boundaries oil−solid and water−solid. It should be noted that the Young equation can be derived based on both energy and force considerations, with the two approaches being equivalent. In particular, the force interpretation of σ_{os} and σ_{ws} stems from the work of Gibbs,[45] who coined the term "superficial tensions" for them. By definition, the superficial tension opposes

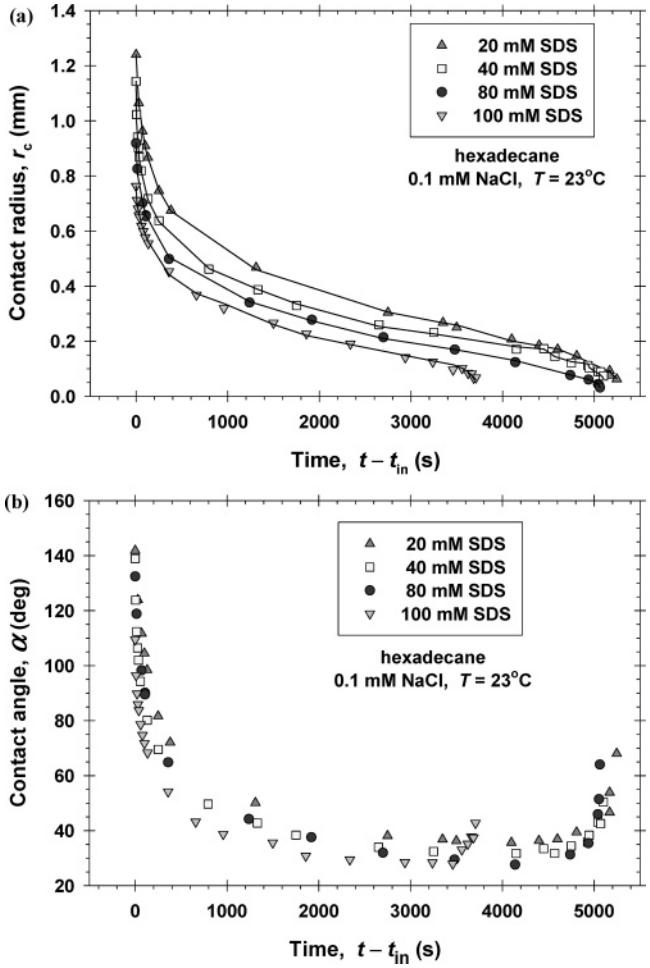

Figure 4. Effect of the SDS concentration on the detachment of hexadecane drops from glass: experimental data (a) for the contact-line radius, r_c, and (b) for the contact angle, α, plotted vs time. The initial moment, t_{in}, corresponds to the first experimental point. The NaCl concentration is 0.1 mM, and the temperature is 23 °C.

every increase of the wet area, without any deformation of the solid, in the same way as σ_{ow} opposes every dilatation of the interface between the two fluids. From this viewpoint, the superficial tensions σ_{os} and σ_{ws} can be interpreted as surface tensions, i.e., *forces* per unit length. Thus, the Young equation has the meaning of a tangential projection of a vectorial force balance per unit length of the contact line. Correspondingly, the normal component of the meniscus surface tension, σ_{ow} sin α, is counterbalanced by the bearing reaction of the solid substrate.

The experimental variation of α (Figures 4−7) is caused by the spontaneous movement of the contact line and decrease of r_c, which, in its own turn, is due to the imbalance of the interfacial tensions at the contact line. The force balance per init length of a *moving* contact line includes also the line viscous friction, which exactly compensates the imbalance of the interfacial tensions under quasi-stationary conditions:[16,37]

$$\beta \frac{dr_c}{dt} = \sigma_{ow} \cos \alpha + \sigma_{ws} - \sigma_{os} \tag{3.2}$$

where β is the line friction coefficient. The appearance of a line friction force, β (dr_c/dt), can be attributed to the circumstance that, during the contact-line motion, oil molecules are taken out of potential wells at the solid

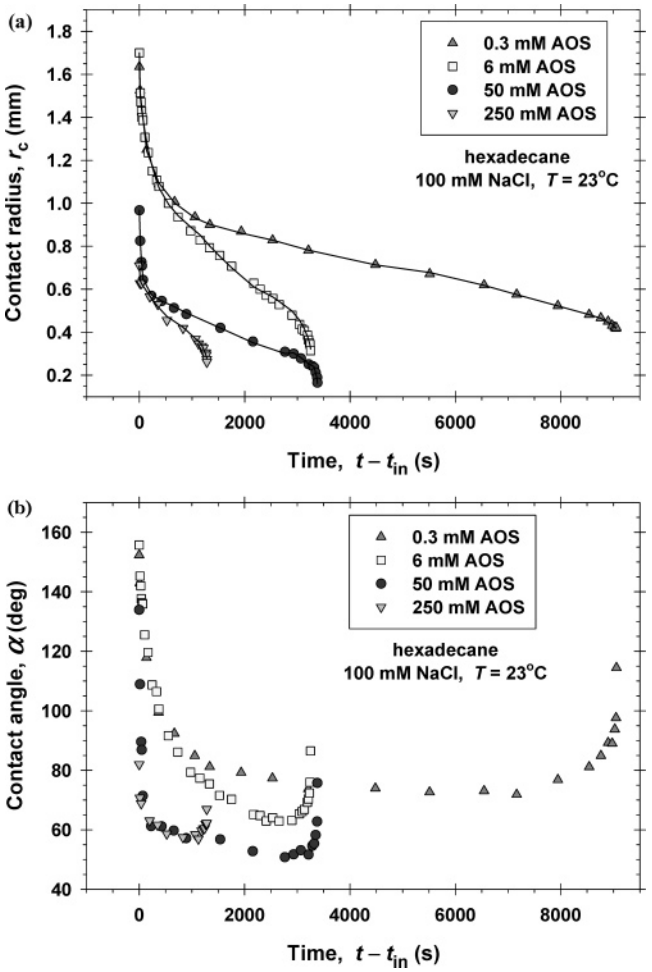

Figure 5. Effect of the AOS concentration on the detachment of hexadecane drops from glass: experimental data (a) for the contact-line radius, r_c, and (b) for the contact angle, α, plotted vs time. The initial moment, t_{in}, corresponds to the first experimental point. The NaCl concentration is 100 mM, and the temperature is 23 °C.

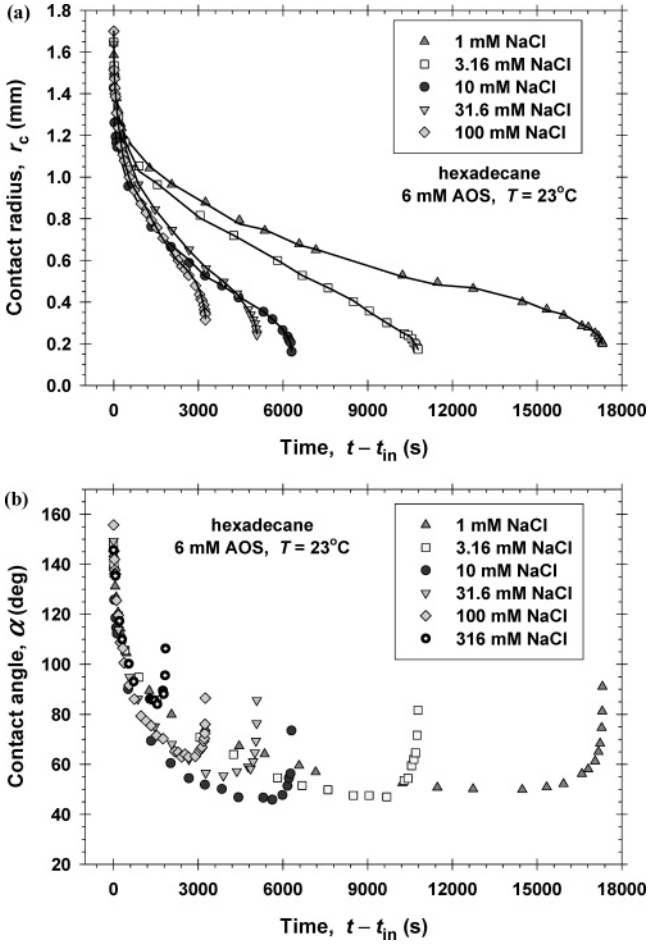

Figure 6. Effect of the NaCl concentration on the detachment of hexadecane drops from glass: experimental data (a) for the contact-line radius, r_c, and (b) for the contact angle, α, plotted vs time. The initial moment, t_{in}, corresponds to the first experimental point. The AOS concentration is 6 mM, and the temperature is 23 °C.

surface and replaced by water molecules, accompanied with dissipation of kinetic energy in the zone of the contact line.[16,35] Note that the imbalance of the interfacial tensions (the right-hand side of eq 3.2) determines the rate of motion of the contact line, dr_c/dt (the left-hand side of eq 3.2). Moreover, if the friction term, β (dr_c/dt), is sufficiently large (as found in our previous study[16]), then it will not allow the imbalance of tensions to relax quickly. Instead, the contact line will move relatively slowly, hindered by the viscous friction.

In ref 16, we established that the data for detaching oil drops agree very well with eq 3.2. Assuming that $\sigma_{ws} - \sigma_{os}$ was constant, we plotted dr_c/dt vs σ_{ow} cos α and obtained a linear dependence. From its slope, we determined the line friction coefficient, β; see eq 3.2. We applied the same relatively simple procedure to the data in Figures 4−7. Unfortunately, we found that in the present case (different glass substrates) the dependence of dr_c/dt on σ_{ow} cos α is not linear; a typical example is shown in Figure 8. The situation is similar for all studied solutions and temperatures.

A closer inspection of Figure 8 reveals the reason for the nonlinear dependence. For the right-hand-side experimental points, we have $dr_c/dt \approx 0$, but the contact angle α continues to vary (σ_{ow} is constant). According to eq 3.2, this could happen only if the difference $\sigma_{os} - \sigma_{ws}$ is not constant but varies with time in the present series of experiments. Such a behavior could be a consequence of the formation of a gel layer on the glass surface in contact with water. The latter idea serves as a basis for the development of a theoretical model in the next section.

4. Theoretical Model

4.1. Physicochemical Background. Let us first consider a possible mechanism of penetration of the oil−glass interface by water as the likely cause of the continuing detachment process. There are many experimental indications that water may dissolve or diffuse into and swell the glass (and silica) surface, forming a surface gel layer.[46−54] This effect has been detected in surface-force measurements[50,52,54] and in experiments on adsorption of macromolecules on glass.[53] As a part of the dissolution process, water may break silicon−oxygen bonds and form a hydroxylated surface.[54] In addition, the formation of a gel layer may include an ion-exchange process, in which protons replace sodium ions at the glass surface.[47,49,53] A swelling of the surface layers has been directly detected with some glasses in a humid atmosphere by analytical methods: the surface area is increased by at least 10 times, micropores appear, and clusters are formed on the interface.[51] Coming back to our system, we could hypothesize that water molecules in the gel layer at the water−glass

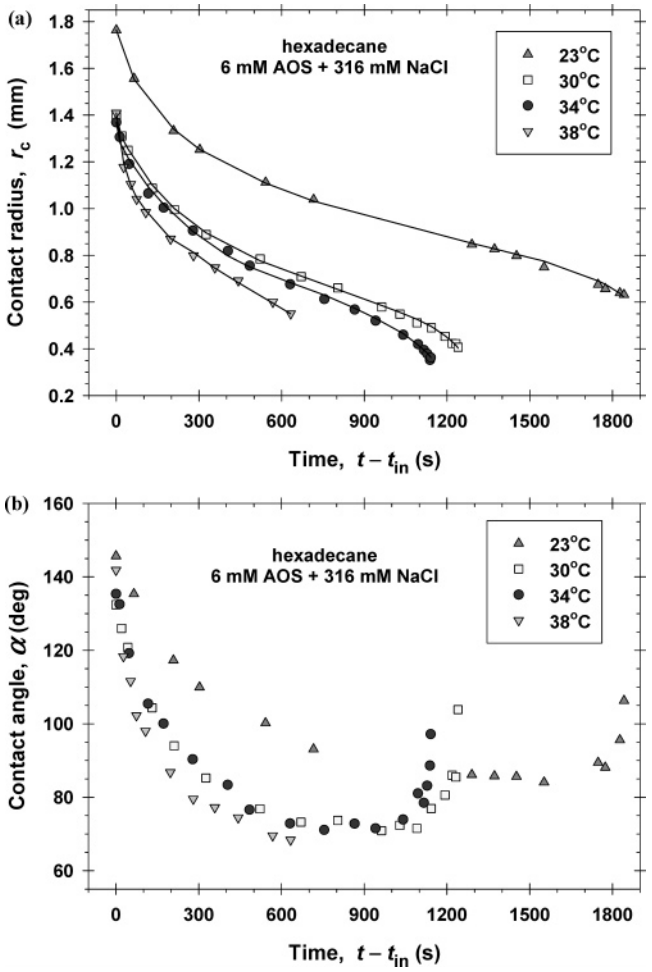

Figure 7. Effect of the temperature on the detachment of hexadecane drops from glass: experimental data (a) for the contact-line radius, r_c, and (b) for the contact angle, α, plotted vs time. The initial moment, t_{in}, corresponds to the first experimental point. The AOS and NaCl concentrations are 6 and 316 mM, respectively.

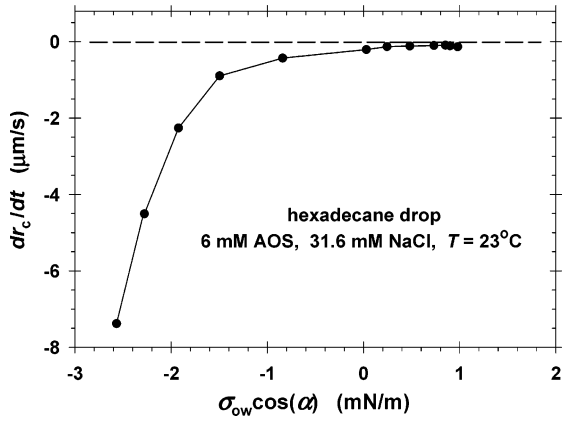

Figure 8. Typical plot of dr_c/dt vs $\sigma_{ow}\cos(\alpha)$: experimental data for a hexadecane drop attached to a glass substrate in a solution of 6 mM AOS + 31.6 mM NaCl at $T = 23$ °C. The line is a guide to the eye.

interface can penetrate, by diffusion, the oil−glass interface, at least in a close vicinity of the contact line (Figure 9). The presence of water molecules in the surface layer of the plate would alter the values of the two superficial tensions, σ_{ws} and σ_{os}, which, in turn, would affect the force balance expressed by the dynamic Young equation, eq 3.2. The resulting uncompensated

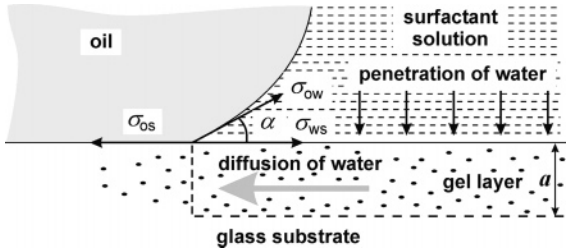

Figure 9. Possible model of the spontaneous detachment of an oil drop from a glass substrate in a surfactant solution. Water molecules from the gel layer at the glass−water interface penetrate by diffusion the glass−oil interface (in the close vicinity of the contact line) and alter the local values of the two superficial tensions, σ_{ws} and σ_{os}, which, in turn, affect the force balance at the contact line.

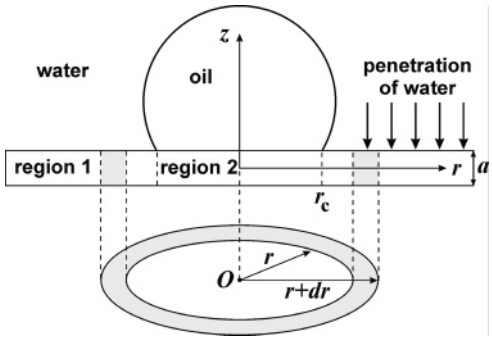

Figure 10. Illustration of eq 4.2, expressing the mass balance of water in the gel layer. The z axis of the coordinate system coincides with the axis of symmetry of the oil drop; r is the radial coordinate, and r_c is the radius of the three-phase contact line.

force would drive the spontaneous shrinking of the contact line. In the following, we give a quantitative description of the water diffusion in the substrate's surface layer (Figure 9).

4.2. Diffusion of Water in the Surface Layer. We introduce a cylindrical coordinate system with a z axis, which coincides with the axis of symmetry of the drop; see Figure 10. We consider a layer of thickness, a, at the solid surface, where the gel layer develops because of penetration of water. This layer could be divided into two separate regions: *region 1* at the water−glass interface ($r_c < r < \infty$) and *region 2* at the oil−glass interface ($0 \le r < r_c$); r is the radial coordinate. We denote by $c_1(r,t)$ and $c_2(r,t)$ the concentrations of water in regions 1 and 2:

$$c(r,t) = \begin{cases} c_1(r,t) & \text{for } r > r_c \\ c_2(r,t) & \text{for } 0 < r < r_c \end{cases} \qquad (4.1)$$

The formation of a gel layer is described as an increase of the concentration of water, $c(r,t)$, with time, t, up to a maximal equilibrium concentration, c_{eq}. In our model, the thickness, a, of the considered thin surface layer is assumed to be constant, and the diffusion of water is supposed to be in the radial direction; i.e., c_1 and c_2 are independent of z.

To quantify the mass balance of water in region 1, we select a ring-shaped volume of the surface layer, which is confined between radii r and $r + dr$ (Figure 10). The variation of the number of water molecules in the considered elementary volume is equal to the algebraic sum of the incoming and outgoing fluxes of water:

$$2\pi r\,\mathrm{d}r\,a\,\frac{\partial c_1}{\partial t} = 2\pi(r+\mathrm{d}r)aQ(r+dr) - 2\pi raQ(r) + 2\pi r\,\mathrm{d}r\,Q_\mathrm{p} \quad (4.2)$$

Here, $Q(r + \mathrm{d}r)$ is the incoming diffusion flux of water through the outer wall of the ring, while $Q(r)$ is the outgoing diffusion flux through the inner wall; Q_p is the influx of water molecules penetrating through the upper boundary of the ring (the water−glass interface). The division of eq 4.2 by $2\pi ar\,\mathrm{d}r$, followed by the transition $\mathrm{d}r \to 0$, yields

$$\frac{\partial c_1}{\partial t} = \frac{1}{r}\frac{\partial}{\partial r}(rQ) + \frac{Q_\mathrm{p}}{a} \quad (4.3)$$

We will use standard expressions for the diffusion and penetration fluxes:[55]

$$Q = D\frac{\partial c_1}{\partial r} \quad (4.4)$$

$$Q_\mathrm{p} = \alpha_\mathrm{m}(c_\mathrm{eq} - c_1) \quad (4.5)$$

where D is the diffusion coefficient, c_eq is the equilibrium concentration of water in the gel layer, and α_m is a mass-transfer coefficient. The substitution of eqs 4.4 and 4.5 into eq 4.3 gives a partial differential equation for $c_1(r,t)$:

$$\frac{\partial c_1}{\partial t} = \frac{D}{r}\frac{\partial}{\partial r}\left(r\frac{\partial c_1}{\partial r}\right) + \frac{1}{t_\mathrm{p}}(c_\mathrm{eq} - c_1) \quad (4.6)$$

which is valid for $r > r_\mathrm{c}$ and $t > 0$; here $t_\mathrm{p} = a/\alpha_\mathrm{m}$.

The mass balance of water in region 2 of the gel layer is similar, with the only difference being that the last term in eq 4.6 is missing because there is no penetration of water through the upper boundary (through the oil−solid interface):

$$\frac{\partial c_2}{\partial t} = \frac{D}{r}\frac{\partial}{\partial r}\left(r\frac{\partial c_2}{\partial r}\right) \qquad (0 \le r \le r_\mathrm{c}) \quad (4.7)$$

($t > 0$). The boundary conditions at the contact line are

$$c_1(r_\mathrm{c},t) = c_2(r_\mathrm{c},t) \equiv c_\mathrm{b}(t) \quad (4.8)$$

$$D\frac{\partial c_1}{\partial r} = D\frac{\partial c_2}{\partial r} \qquad \text{at } r = r_\mathrm{c} \quad (4.9)$$

Here $c_\mathrm{b}(t)$ is the concentration of water molecules at the boundary, $r = r_\mathrm{c}$, between the regions 1 and 2; eq 4.9 expresses the equality of the diffusion fluxed at this boundary. We have two additional boundary conditions at infinity and at the axis of symmetry:

$$\left.\frac{\partial c_1}{\partial r}\right|_{r\to\infty} = 0, \quad \left.\frac{\partial c_2}{\partial r}\right|_{r=0} = 0 \quad (4.10)$$

Moreover, we assume that at the initial moment, $t = 0$, there was no water in the considered layer on the solid surface.

First, let us find the asymptotics of $c_1(r,t)$ far from the contact line ($r \gg r_\mathrm{c}$), where the diffusion term in eq 4.6 (that containing D) is negligible. In this limiting case, the solution of eq 4.6 reads

$$c_1 \approx c_\mathrm{eq}[1 - \exp(-t/t_\mathrm{p})] \equiv c_\infty(t) \qquad (r \gg r_\mathrm{c}) \quad (4.11)$$

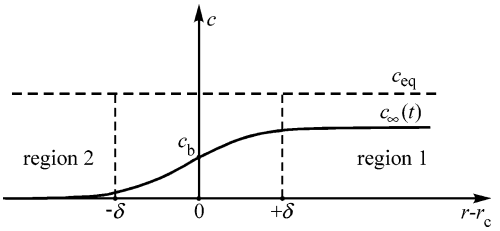

Figure 11. Schematic dependence of the concentration of water in the surface layer of glass, c, on the distance to the contact line, $r - r_\mathrm{c}$. c_b is the value of c at the contact line; the latter serves as the boundary between regions 1 and 2; δ characterizes the width of the transition zone between the two regions; $c_\infty(t)$ is the limiting value of c in region 1, far from the transition zone; c_eq is the value of c for a glass surface, which is equilibrated with water.

See Figure 11 for the notation. In the limit $t \to \infty$, eq 4.11 gives $c_1 \to c_\mathrm{eq}$, which means that eventually the gel layer equilibrates with the water phase.

To find the variation of c_1 close to the contact line, it is convenient to introduce the auxiliary function:

$$c_{1\delta}(r,t) \equiv c_1(r,t) - c_\infty(t) \quad (4.12)$$

where $c_\infty(t)$ is defined by eq 4.11. The substitution of eq 4.12 into eq 4.6 yields the following simpler equation for $c_{1\delta}$:

$$\frac{\partial c_{1\delta}}{\partial t} = \frac{D}{r}\frac{\partial}{\partial r}\left(r\frac{\partial c_{1\delta}}{\partial r}\right) - \frac{c_{1\delta}}{t_\mathrm{p}} \quad (4.13)$$

The major variation of the concentration of water in the considered surface layer happens in the vicinity of the contact line (around the point $r - r_\mathrm{c} = 0$ in Figure 11). Let us denote the characteristic width of this zone by δ. To describe the variation of $c_{1\delta}$ there, it is convenient to replace the variables r and t with new variables x and τ as follows:

$$x = [r - r_\mathrm{c}(t)]/\delta; \quad \tau = t/\delta^2 \quad (4.14)$$

In terms of the new variables, the derivative in the left-hand side of eq 4.13 can be expressed as follows:

$$\left(\frac{\partial c_{1\delta}}{\partial t}\right)_r = \left(\frac{\partial c_{1\delta}}{\partial \tau}\right)_x\left(\frac{\partial \tau}{\partial t}\right)_r + \left(\frac{\partial c_{1\delta}}{\partial x}\right)_\tau\left(\frac{\partial x}{\partial t}\right)_r \quad (4.15)$$

Then, with the help of eqs 4.14 and 4.15, we can represent eq 4.13 in the form

$$\frac{\partial c_{1\delta}}{\partial \tau} = \delta\frac{\mathrm{d}r_\mathrm{c}}{\mathrm{d}t}\frac{\partial c_{1\delta}}{\partial x} + D\frac{1}{1 + x\delta/r_\mathrm{c}}\frac{\partial}{\partial x}\left[(1 + x\delta/r_\mathrm{c})\frac{\partial c_{1\delta}}{\partial x}\right] - \frac{\delta^2}{t_\mathrm{p}}c_{1\delta} \quad (4.16)$$

We do not know in advance the value of the diffusivity, D, of water in the gel layer. For this reason, we checked (against the experimental data) the predictions of different versions of the model: with fast, slow, and stationary diffusion. It turned out that only the case of *fast* diffusion (eq 4.17) compares well with the experiment. In this case, the characteristic diffusion rate, D/δ, is much greater than the rate of contact-line motion, $\mathrm{d}r_\mathrm{c}/\mathrm{d}t$, which leads to a small width, δ, of the transitional zone around the contact line and to a small value of the ratio δ/t_p:

$$\frac{dr_c}{dt} \ll \frac{D}{\delta}; \quad \frac{\delta}{r_c} \ll 1; \quad \frac{\delta}{t_p} \ll \frac{D}{\delta} \tag{4.17}$$

In view of the latter relationships, eq 4.16 acquires the following simpler approximate form:

$$\frac{\partial c_{1\delta}}{\partial \tau} = D\frac{\partial^2 c_{1\delta}}{\partial x^2} \qquad (x \geq 0) \tag{4.18}$$

Likewise, using eqs 4.14 and 4.17, we present eq 4.7 in the form

$$\frac{\partial c_2}{\partial \tau} = D\frac{\partial^2 c_2}{\partial x^2} \qquad (x \leq 0) \tag{4.19}$$

With the help of the Laplace transform, from eqs 4.18 and 4.19, we derive

$$\tilde{c}_{1\delta} = -\tilde{c}_b \exp(-x\sqrt{s/D}), \quad \tilde{c}_2 = \tilde{c}_b \exp(x\sqrt{s/D}) \tag{4.20}$$

where the Laplace transforms are denoted by a tilde

$$\tilde{c}_{1\delta}(x,s) \equiv L[c_{1\delta}(x,\tau)], \quad \tilde{c}_2(x,s) \equiv L[c_2(x,\tau)], \quad \tilde{c}_b(s) \equiv L[c_b(t)] \tag{4.21}$$

Here s is the Laplace parameter and, as before, $c_b(t)$ is the boundary concentration at the contact line ($x = 0$); see eq 4.8. To obtain eq 4.20, we used the boundary condition $c_2(x=0) = c_b$ and the equality of the diffusion fluxes, eq 4.9. Next, we transform the definition of $c_{1\delta}$, eq 4.12, and in the result we substitute $x = 0$:

$$\tilde{c}_{1\delta}(0,s) = \tilde{c}_b(s) - L[c_\infty(t)] \tag{4.22}$$

On the other hand, setting $x = 0$ in eq 4.20, we get $\tilde{c}_{1\delta}(0,s) = -\tilde{c}_b(s)$. Substituting the latter expression into eq 4.22, we obtain $\tilde{c}_b(s) = 0.5L[c_\infty(t)]$. Finally, we apply the inverse Laplace transformation and substitute eq 4.11:

$$c_b(t) = \frac{1}{2}c_\infty(t) = \frac{c_{eq}}{2}\left[1 - \exp\left(-\frac{t}{t_p}\right)\right] \tag{4.23}$$

In principle, eq 4.23, together with eq 4.20, gives the solution of the considered diffusion problem. Because we are interested in the force balance at the contact line, it turns out that eq 4.23 is sufficient to quantify the effect of water diffusion on the contact-line motion. We recall that eq 4.23 is derived for the case of slow motion and a narrow transition zone (see eq 4.17), which corresponds to our experimental situation. (The latter fact is checked by comparing the theoretical model with the experiment; see the following.)

4.3. Description of the Contact-Line Motion. In general, the superficial tensions, σ_{ws} and σ_{os}, depend on the concentration of water molecules, c_b, in the surface layer at the contact line. To quantify the latter dependence, we will assume that the simple Henry law for surface tensions is satisfied:

$$\sigma_{ws} = \sigma_{ws}(0) - \lambda_{ws}c_b, \quad \sigma_{os} = \sigma_{os}(0) + \lambda_{os}c_b \tag{4.24}$$

where $\sigma_{ws}(0)$ and $\sigma_{os}(0)$ are the respective values for a dry solid surface, while λ_{ws} and λ_{os} are coefficients of proportionality. The substitution of eqs 4.23 and 4.24 into the equation for contact-line motion, eq 3.2, yields

$$\beta\frac{dr_c}{dt} = \sigma_{ow}\cos\alpha(t) - \Delta\sigma + \gamma\exp\left(-\frac{t}{t_p}\right) \tag{4.25}$$

where we have introduced the notation

$$\gamma \equiv (\lambda_{ws} + \lambda_{os})(c_{eq}/2) \tag{4.26}$$

$$\Delta\sigma \equiv \sigma_{os}(0) - \sigma_{ws}(0) + (\lambda_{os} + \lambda_{ws})(c_{eq}/2) \tag{4.27}$$

γ and $\Delta\sigma$ are parameters of our model. Note that in view of eqs 4.24 and 4.27 we have

$$\Delta\sigma \equiv \sigma_{os}(c_{eq}/2) - \sigma_{ws}(c_{eq}/2) \tag{4.28}$$

i.e., $\Delta\sigma$ is the difference between the superficial tensions for a half-equilibrated surface layer of glass. (The relative importance of the three terms in the right-hand side of eq 4.25 is discussed in section 5.2.) Furthermore, we recall that the dependence $\alpha(t)$ is known from the experiment; see Figures 4b−7b. Then, eq 4.25 can be integrated to derive the theoretical time dependence of the contact-line radius:

$$r_c(t) = r_c(0) + \frac{\sigma_{ow}}{\beta}\int_0^t \cos\alpha(\hat{t})\,d\hat{t} - \frac{\Delta\sigma}{\beta}t + \frac{\gamma t_p}{\beta}\left[1 - \exp\left(-\frac{t}{t_p}\right)\right] \tag{4.29}$$

where $r_c(0)$ is the contact-line radius at the initial moment, $t = 0$; $\hat{t}$ is an integration variable.

5. Comparison of Theory and Experiment

5.1. Principles of the Procedure for Data Processing. We do not know the experimental value $r_c(0)$ because some time (different in different runs) elapses between the moment $t = 0$ (when the solution has been poured in the experimental cell) and the initial moment, t_{in}, when the video recording of the drop detachment has started. This difficulty can be overcome by a special construction of the procedure of data processing, as explained in the following. First, we substitute $t = t_{in}$ into eq 4.29 and subtract the result from eq 4.29:

$$r_c(t_{in} + \Delta t) = r_c(t_{in}) + \frac{\sigma_{ow}}{\beta}\int_0^{\Delta t}\cos\alpha(\hat{t})\,d\hat{t} - \frac{\Delta\sigma}{\beta}\Delta t + A\frac{t_p}{\beta}\left[1 - \exp\left(-\frac{\Delta t}{t_p}\right)\right] \tag{5.1}$$

$$\Delta t \equiv t - t_{in}, \quad A = \gamma\exp(-t_{in}/t_p) \tag{5.2}$$

Here, Δt is the experimental time: we have $\Delta t = 0$ at the moment of the beginning of video recording. The experimental points in Figures 4a−7a have coordinates $(\Delta t_i, r_i^{exp})$, where r_i^{exp} is the experimental value of r_c at the moment Δt_i. The corresponding theoretical value, $r_i^{th} = r_c(t_{in} + \Delta t_i)$, is given by eq 5.1. The contact-line radius at the initial moment, $r_c(t_{in})$, the oil−water interfacial tension, σ_{ow}, and the contact angle, $\alpha(t)$, are known from the experiment. Thus, four unknown parameters remain in eq 5.1: β, $\Delta\sigma$, A, and t_p. They can be determined from the best fit of the experimental dependence r_c vs Δt. With this goal, it is convenient to represent eq 5.1 in the following form:

$$r_i^{\text{th}} = r_c^{\text{exp}}(t_{\text{in}}) + b_1F_1(\Delta t_i) + b_2F_2(\Delta t_i) + b_3F_3(\Delta t_i) \quad (5.3)$$

($i = 1, 2, ..., N$), where $b_1 \equiv \sigma_{ow}/\beta$, $b_2 \equiv \Delta\sigma/\beta$, and $b_3 \equiv At_p/\beta$ are adjustable parameters, N is the number of experimental points, and F_1, F_2, and F_3 are functions defined as follows:

$$F_1(\Delta t) \equiv \int_0^{\Delta t} \cos\alpha(t)\, dt, \quad F_2(\Delta t) \equiv -\Delta t, \quad F_3(\Delta t) \equiv 1 - \exp[-\Delta t/t_p] \quad (5.4)$$

The values of F_1 were calculated for each Δt_i from the experimental data for the contact angle α vs time in Figures 4b−7b; the trapezium rule for numerical integration was employed.[56]

To fit a given experimental curve, r_c vs Δt, like those in Figures 4a−7a, we first assume a tentative value of the parameter t_p. With the latter value, we calculate $F_3(\Delta t_i)$ by eq 5.4. Next, applying the least-squares method, we consider the following merit function:

$$\Phi(b_1,b_2,b_3,t_p) = \sum_{i=1}^{N}[r_i^{\text{exp}} - r_i^{\text{th}}(b_1,b_2,b_3,t_p)]^2 \quad (5.5)$$

The fit of the data is facilitated by the fact that r_i^{th}, given by eq 5.3, is a linear function of the parameters b_1, b_2, and b_3. The values of the latter three parameters, which minimize Φ (for a given t_p), can be obtained as the solution of the following linear system of three equations:

$$\sum_{j=1}^{3}[\sum_{i=1}^{N}F_j(\Delta t_i)\, F_k(\Delta t_i)]b_j = \sum_{i=1}^{N}F_k(\Delta t_i)\, [r_i^{\text{exp}} - r_c^{\text{exp}}(t_{\text{in}})] \quad (5.6)$$

($k = 1-3$). We solve this linear system directly, using Cramer's rule. Thus, we determine $b_1(t_p)$, $b_2(t_p)$, and $b_3(t_p)$. Now, eq 5.5 gives Φ as a function of a single parameter, t_p. The resulting function $\Phi(t_p)$ is minimized numerically by means of the Levenberg−Marquardt method.[57] Finally, we calculate the parameters of the model:

$$\beta = \sigma_{ow}/b_1, \quad \Delta\sigma = \beta b_2, \quad A = \beta b_3/t_p \quad (5.7)$$

For all processed experimental curves, the minimum of $\Phi(t_p)$ was well pronounced and accurately determined. This is an argument in favor of the adequacy of our theoretical model. Another argument is the behavior of the determined adjustable parameters (for different, independently processed experimental curves r_c vs Δt) as functions of the temperature and surfactant and salt concentrations.

The results from the data fits are reported in the next subsection. Let us mention in advance that, by definition, the parameter A depends on the randomly defined initial moment, t_{in}; see eq 5.2. For this reason, the values of A should be scattered; i.e., they are not expected to depend systematically on the temperature and surfactant and salt concentrations. In fact, this is what we obtained for A from the fits. In contrast, β, t_p, and $\Delta\sigma$ are physical parameters, which are expected to depend in a systematic manner on the temperature and surfactant and salt concentrations. The latter anticipation is confirmed by the results from the fits (see Tables 1−4).

Table 1. Effect of the SDS Concentration on the System Parameters at 0.1 mM NaCl and 23 °C

SDS (mM)	σ_{ow} (mN/m)	β (Pa·s)	t_p (s)	$\Delta\sigma$ (μN/m)	st. dev. (mm)
20[a]	7.7	20.7	1568	38.1	0.032
20[b]	7.7	20.9	1582	38.0	0.028
40	7.5	18.1	1100	38.4	0.026
80	7.4	15.2	745	38.2	0.029
100	7.5	15.1	691	38.9	0.028

[a] Drop of volume of 0.7415 mm^3. [b] Drop of volume of 1.142 mm^3.

Table 2. Effect of the AOS Concentration on the System Parameters at 100 mM NaCl and 23 °C

AOS (mM)	σ_{ow} (mN/m)	β (Pa·s)	t_p (s)	$\Delta\sigma$ (μN/m)	st. dev. (mm)
0.3	3.7	14.9	2450	4.40	0.027
6	3.6	3.2	1240	7.36	0.024
50	3.6	2.0	501	7.46	0.016
250	3.6	1.6	261	7.56	0.017

Table 3. Effect of the NaCl Concentration on the System Parameters at 6 mM AOS and 23 °C

NaCl (mM)	σ_{ow} (mN/m)	β (Pa·s)	t_p (s)	$\Delta\sigma$ (μN/m)	st. dev. (mm)
1	6.6	48.7	4457	30.4	0.027
3.16	5.8	35.3	3635	25.0	0.024
10	5.1	20.2	1784	19.2	0.025
31.6	4.4	9.0	1325	13.4	0.023
100	3.6	3.2	1240	7.4	0.024
316	2.9	3.1	1200	4.2	0.022

Table 4. Effect of the Temperature on the System Parameters at 6 mM AOS and 316 mM NaCl

T (°C)	σ_{ow} (mN/m)	β (Pa·s)	t_p (s)	$\Delta\sigma$ (μN/m)	st. dev. (mm)
20	3.10	5.46	2414	5.93	0.030
23	2.94	3.10	1200	4.20	0.022
25	2.86	3.04	1168	4.32	0.026
30	2.74	2.92	946	4.50	0.014
34	2.58	2.34	797	4.46	0.022
38	2.47	0.38	245	2.70	0.023

5.2. Numerical Results and Discussion. As mentioned above, the points (symbols) in Figures 4a−7a denote the experimental r_c while the solid lines connect the respective theoretical values of r_c, obtained by fitting the data as described in section 5.1. Figures 4a−7a indicate excellent agreement between the theoretical model and the experiment. This is seen also from the relatively small values of the standard deviation of the fits, which is given in the last columns of Tables 1−4. The standard deviation is $(\Phi_{\text{min}}/N)^{1/2}$, where Φ_{min} is the minimum value of Φ, corresponding to the best fit (see eq 5.5).

The values of the hexadecane−water interfacial tension, σ_{ow}, given in Tables 1−4, are used as input parameters when fitting the data for r_c vs time. As explained in section 2, σ_{ow} was determined by fitting the drop profile with the Laplace equation (see Figure 3). From different photographs of the same drop at different stages of detachment (like those in Figure 2), we determined the same value of σ_{ow}, which can be identified as the equilibrium σ_{ow}. In other words, the dynamics of surfactant adsorption at the oil−water interface is so fast that this process ends before the beginning of our measurements. In addition, the variation of the oil−water area during the drop detachment is much slower than the rate of establishment of adsorption−desorption equilibrium at the oil−water interface. This is evidenced also from the constancy of

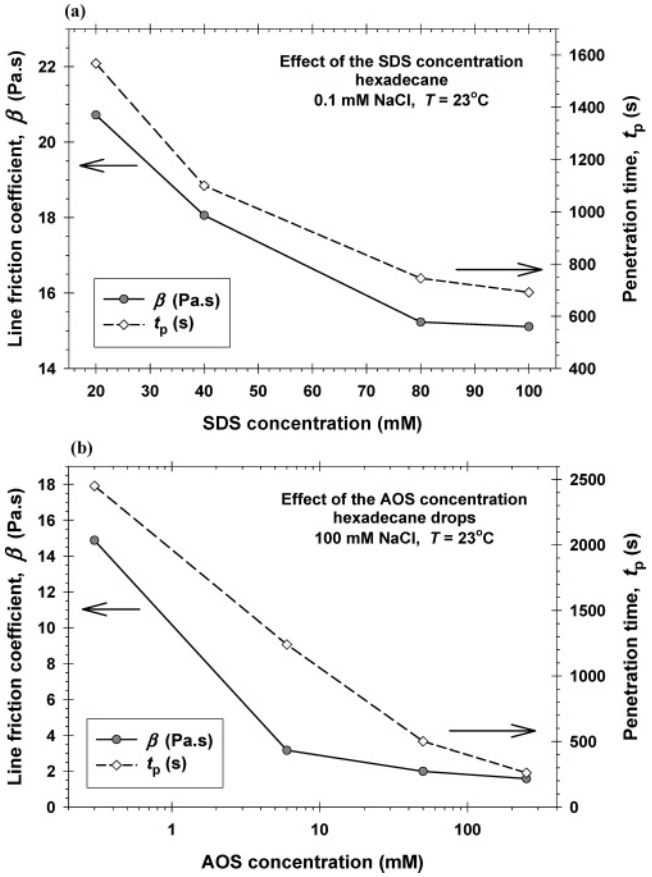

Figure 12. Effect of the surfactant concentration on the line friction coefficient, β, and penetration time, t_p: (a) solutions of SDS with 0.1 mM NaCl; (b) solutions of AOS with 100 mM NaCl. The values of β and t_p are determined from the fits of experimental data for hexadecane drops at a temperature of 23 °C.

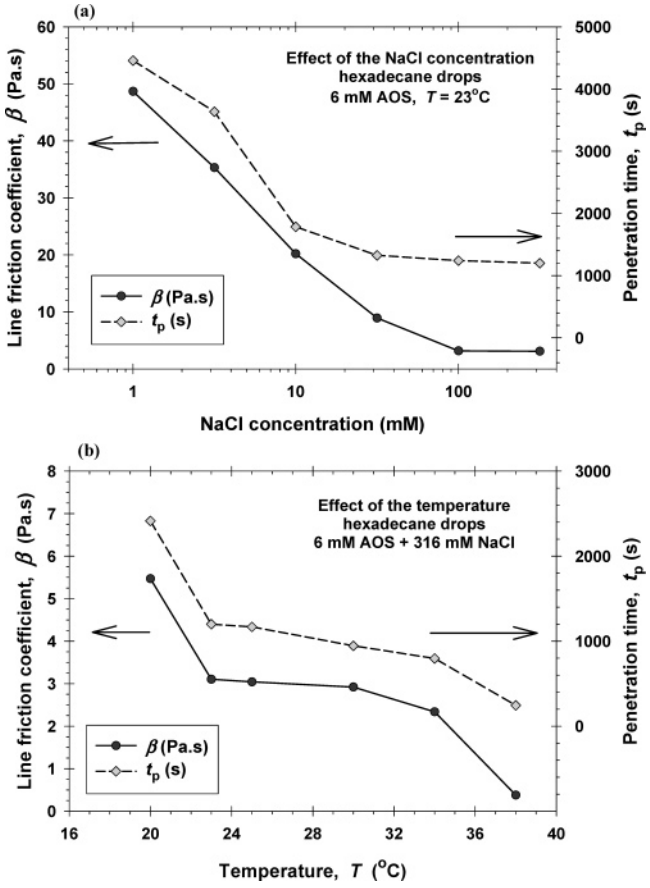

Figure 13. Line friction coefficient, β, and penetration time, t_p, determined from the fits of experimental data for hexadecane drops in aqueous solutions containing 6 mM AOS: (a) effect of the NaCl concentration at $T = 23$ °C; (b) effect of the temperature at fixed NaCl concentration, 316 mM.

σ_{ow} in Tables 1 and 2, at various surfactant concentrations. Such a behavior is typical for the surface/interfacial tension of surfactant solutions above the critical micelle concentration (cmc); see, e.g., ref 58. It is well-known that the kinetics of surfactant adsorption is very fast above the cmc. One can check that the data in Table 3 imply that σ_{ow} decreases linearly with the rise of $\ln(C_{NaCl})$, which is also a typical behavior due to adsorption of Na^+ counterions; see, e.g., ref 59 [C_{NaCl} is the concentration of NaCl]. Finally, the data in Table 4 indicate that σ_{ow} decreases linearly with the rise of temperature, as should be expected.[17]

As noted above, all experiments have been carried out with hexadecane drops, whose volume was different in different runs. The values of the parameters β, t_p, and $\Delta\sigma$, determined from the best fits, turned out to be independent of the drop volume, as must be expected, having in mind the physical meaning of these parameters (see above). As an illustration, the first two rows of Table 1 compare data for two hexadecane drops of different volumes, with all other experimental conditions being the same. One sees that the determined β, t_p, and $\Delta\sigma$ have very close values for these two drops.

In fact, here we present the first systematic measurements of the line friction coefficient, β, for solid−water−oil systems. In our previous study,[16] $\beta = 1.6$ Pa·s was determined at some specific experimental conditions for a glass−water−oil system. Values of β of the same order, as well as greater values, are determined in our present study, depending on the experimental conditions; see Tables 1−4 and Figures 12 and 13. To the best of our knowledge, the only other experimental value of the line friction coefficient, so far mentioned in the literature, is $\beta \approx 4.5$ Pa·s, which was determined in ref 39 for water drops (with 75% dissolved glycerol) that are spreading over a Teflon substrate (the third phase is air).

The data in Tables 1 and 2 show that the line friction coefficient, β, and the penetration time of water into the surface layer of glass, t_p, decrease with the rise of the surfactant concentration. This effect is very pronounced in Table 2: both β and t_p decrease 9.3 times when the AOS concentration is increased from 0.3 to 250 mM. Likewise, the data in Table 3 indicate that β and t_p decrease also with the rise of the NaCl concentration: β decreases about 16 times and t_p about 4 times when the salt concentration rises from 1 to 316 mM. It is remarkable also that β and t_p vary in a similar manner when the temperature and surfactant and salt concentrations are varied; see Figures 12 and 13.

The above results about the behavior of β and t_p call for a more detailed discussion. The correlation between β and t_p (Figures 12 and 13) is not so surprising because both β and t_p are related to the penetration of water in the surface layer of the solid substrate. In particular, water molecules penetrating in the three-phase contact zone displace the adsorbed oil molecules from their potential wells on the solid surface, and thus the contact line advances. The surfactant molecules facilitate the detachment of the oil from the glass surface because they cover the newly formed oil−water interface (in the zone of three-phase contact) and decrease its surface free

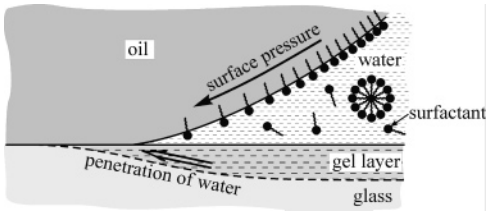

Figure 14. Surfactant molecules, which facilitate the detachment of the oil from the glass surface because they cover the newly formed oil−water interface (in the zone of three-phase contact) and decrease its surface free energy.

energy (Figure 14). The added salt suppresses the electrostatic repulsion between the surfactant ions and thus increases the rate of surfactant adsorption, as well as the equilibrium adsorption. This could be a possible explanation for the decrease of the friction coefficient β with the rise of the surfactant and salt concentrations (Figures 12 and 13).

On the other hand, t_p is a property of the interface solid−water, unlike β, which is characteristic of the three-phase contact zone. The bare glass−water interface is negatively charged,[60] and the anionic surfactants do not adsorb on glass. For this reason, it seems unclear how the surfactant and salt could affect the penetration time of water in the surface layer of glass, t_p. We could propose two possible explanations.

First, experiments show that a thin hydrophobic layer, some kind of gloss, covers the surface of the commercial glass slides used. Indeed, the initial contact angle in our experiments is 140−160° (hydrophobic substrate); see Figures 4b−7b and the first photograph in Figure 2. This hydrophobic coverage can be removed by immersion of the slide in sulfochromic acid. However, the acid-treated glass plates became so hydrophilic that the adherent hexadecane drops detached very fast after pouring the surfactant solution into the experimental cell (Figure 1). Such hydrophilic plates were inappropriate for our experiments because we were unable to record a regular process of drop detachment, like that in Figure 2, because of the high speed of the process. For this reason, we used the slides as received directly from the manufacturer, without any previous treatment. Hence, the detected effect of the surfactant and salt on the water-penetration time, t_p, is most probably related to their role for hydrophilization or removal of the hydrophobic coverage on the glass surface.

Second, after the retreat of the oil, some oil molecules could remain adsorbed at the glass−water interface. The surfactant micelles should solubilize that residual oil, thus accelerating the penetration of water into the surface layer of glass. Moreover, it is known that the salt lowers the electrostatic barrier to micelle contact with the oil and promotes the solubilization process.[43]

Our model is not in conflict with the model by Garoff et al.[31] about a possible carryover of surfactant ahead of the contact line. Indeed, when water molecules penetrate along the boundary between solid and oil (Figure 14), surfactant molecules could also enter the formed thin water film to decrease its surface energy against the oil. Note that oil drops can detach from a glass substrate even in pure water (without any surfactant), but the process is slower. Hence, in our case, the presence of surfactant is not a precondition for penetration of water molecules between glass and oil, but when present, the surfactant accelerates this process. On the other hand, if the substrate is essentially hydrophobic and there is no development of a gel layer, the presence of surfactant in the water phase, and its carryover ahead of the contact line,[31] could be a necessary condition for the occurrence of spontaneous drop detachment.

The effect of the temperature on the line friction coefficient, β, and the water-penetration time, t_p (Table 4 and Figure 13b), is easier to understand, insofar as the temperature is known to reduce the viscous effects and accelerate the diffusion processes. In our specific experiment, the rise of the temperature from 20 to 38 °C decreases 14 times β and reduces 10 times t_p (Table 4). This is a considerable effect, which demands the drop-detachment experiments to be carried out in a thermostated cell in order to get reproducible results.

Finally, the difference, $\Delta\sigma$, between the superficial tensions, defined by eq 4.28, turns out to be rather small, between 3 and 39 μN/m; see Tables 1−4. Because $\Delta\sigma$ was determined from the coefficients of the linear fit with the help of eq 5.3, we were able to estimate its experimental error. The estimate indicates that the obtained $\Delta\sigma$ values are reliable, irrespective of their low magnitude. The determined relative errors of β and $\Delta\sigma$ are typically about 1%. For example, for the last line of Table 4 (that with the smallest β and $\Delta\sigma$), we estimated $\beta = 0.379 \pm 0.004$ Pa·s and $\Delta\sigma = 2.70 \pm 0.02$ μN/m.

The fact that we are able to determine $\Delta\sigma$ accurately from the experimental data indicates that $\Delta\sigma$, despite its small value, has an essential effect on the contact-line motion. Indeed, taking values $\Delta\sigma \approx 38$ μN/m and $\beta \approx 20$ Pa·s from Table 1, we obtain $\Delta\sigma/\beta \approx 1.9$ μm/s. If this term were dominating the variation of the contact-line radius, r_c (see eq 4.25), we would have $\Delta r_c \approx (\Delta\sigma/\beta)\Delta t = 7.6$ mm for $\Delta t = 4000$ s; see Figure 4a. However, the typical variation Δr_c in our experiments is about 10 times smaller (Figure 4a). Hence, the negative term with $\Delta\sigma$ in eq 4.25 is to a great extent counterbalanced by the two other terms in eq 4.25, both of them being positive for $\alpha < 90°$. In other words, the three terms in the right-hand side of eq 4.25 have the same order of magnitude, and none of them can be neglected.

The value of $\Delta\sigma$ indicates what would be the equilibrium contact angle at the half-developed gel layer (see eqs 3.2 and 4.28):

$$\cos \alpha_{1/2} = \Delta\sigma/\sigma_{ow} \tag{5.8}$$

Because $\Delta\sigma/\sigma_{ow} \ll 1$, eq 5.8 implies that $\alpha_{1/2} \approx 90°$. As seen in Figure 2, the experimental, nonequilibrium contact angle is $\alpha > 90°$ at the earlier stages of drop detachment, while $\alpha < 90°$ at the later stages. Unfortunately, we cannot determine the parameters in eq 4.24 from our fit, and consequently we could not determine the equilibrium contact angle at the fully developed gel layer ($c = c_{eq}$). If eventually a water film is formed between the glass and oil, then the equilibrium value of α would be very small, close to zero.

6. Summary and Conclusions

In the present paper, we report experimental data and the theoretical model for the dynamics of the detachment of hexadecane drops from a solid substrate (glass plate) in aqueous solutions containing anionic surfactant and salt. The influences of temperature and surfactant and salt concentrations on the motion of the three-phase contact line (solid−water−oil), and on the dynamic contact angle, are investigated (Figures 4−7). We found

that the three factors mentioned considerably affect the detachment process.

A drift (decrease) of the quasi-equilibrium contact angle (Figure 8) indicates that the surface of the solid plate becomes increasingly hydrophilic upon contact with the water phase. This result gave a clue that helped us to find a possible explanation of the experimental facts. Indeed, our data indicate that hydrophilization of the initially hydrophobic thin-layer coverage of the glass slides used occurs in contact with the surfactant solution. In addition, the penetration of water could lead to the formation of a gel layer on the glass surface. In both cases, water molecules can propagate by lateral diffusion in a thin layer on the surface of the solid plate (Figures 9 and 10). Thus, water molecules could penetrate also along the oil−solid boundary, as has been supposed in previous studies.[15] The imbibition of water by the substrate alters the solid−oil and solid−water interfacial tensions in the zone of a three-phase contact (eq 4.24). Consequently, the balance of tensions at the contact line will also be affected. Under dynamic conditions, this balance involves the line friction force, β (dr_c/dt); see eq 3.2.

In this way, the developed theoretical model contains two kinetic parameters: the line friction coefficient, β, and the characteristic time, t_p, of water penetration into the substrate's surface layer. The contact-line velocity is determined by the interplay of these two effects: The driving force of the detachment process, viz., the imbalance of the interfacial tensions at the contact line, is engendered by the water penetration, while the line friction force compensates this imbalance and determines the stationary speed (eq 4.25). First, we solved the problem about the lateral diffusion of water in the substrate's surface layer and derived a useful formula for the water concentration in the contact-line zone (eq 4.23). Next, the dynamic Young equation (eq 4.25) was integrated to determine the theoretical dependence of the contact-line radius on time, $r_c(t)$; see eq 4.29. The latter is employed to fit the experimental data and to determine β and t_p as adjustable parameters (Tables 1−4).

Excellent agreement between the theory and experiment has been achieved (Figures 4a−7a). The obtained parameter values exhibit a systematic dependence on the temperature and surfactant and salt concentrations (Figures 12 and 13) that can be interpreted in the frame of the proposed model (section 5.2). In conclusion, the present study specifies the parameters that can be used to quantitatively characterize the rate of drop detachment, determines the values of these parameters at various experimental conditions, and indicates tools for control of the investigated spontaneous process.

Acknowledgment

This work was supported in part by the program Cooperation and Networking for Excellence (CONEX), financed by the Austrian Ministry of Education, Science and Culture, and in part by Colgate−Palmolive. The authors are indebted to reviewer II for his valuable comments and to Mariana Paraskova for her assistance in the figure preparation.

Literature Cited

(1) Dussan, V. E. B.; Rame, E.; Garoff, S. On Identifying the Appropriate Boundary Conditions at a Moving Contact Line: An Experimental Investigation. *J. Fluid Mech*. **1991**, *230*, 97.

(2) Haley, P. J.; Miksis, M. J. Dissipation and Contact Line Motion. *Phys. Fluids A* **1991**, *3*, 487.

(3) Brochard-Wyart, F.; de Gennes, P. G. Dynamics of Partial Wetting. *Adv. Colloid Interface Sci.* **1992**, *39*, 1.

(4) Shikhmurzaev, Y. D. The Moving Contact Line in a Smooth Solid Surface. *Int. J. Multiphase Flow* **1993**, *19*, 589.

(5) Ruckenstein, E. The Moving Contact Line of a Droplet on a Smooth Solid. *J. Colloid Interface Sci.* **1995**, *170*, 284.

(6) Savelski, M. J.; Shetty, S. A.; Kolb, W. B.; Cerro, R. L. Flow Patterns Associated with the Movement of a Solid/Liquid/Fluid Contact Line. *J. Colloid Interface Sci.* **1995**, *176*, 117.

(7) Neumann, A. W.; Rame, E.; Garoff, S. Experimental Studies on the Parameterization of Liquid Spreading and Dynamic Contact Angles. *Colloids Surf. A* **1996**, *116*, 115.

(8) Blake, T. D.; Clarke, A.; de Coninck, J.; de Ruijter, M. J. Contact Angle Relaxation during Droplet Spreading: Comparison between Molecular Kinetic Theory and Molecular Dynamics. *Langmuir* **1997**, *13*, 2164.

(9) Petrov, J. G.; Ralston, J.; Hayes, R. A. Dewetting Dynamics on Heterogeneous Surfaces. A Molecular-Kinetic Treatment. *Langmuir* **1999**, *15*, 3365.

(10) Blake, T. D.; de Coninck, J. The Influence of Solid−Liquid Interactions on Dynamic Wetting. *Adv. Colloid Interface Sci.* **2002**, *96*, 21.

(11) Starov, V. M.; Kostvintsev, S. R.; Sobolev, V. D.; Velarde, M. G.; Zhdanov, S. A. Spreading of Liquid Drops over Dry Porous Layers: Complete Wetting Case. *J. Colloid Interface Sci.* **2002**, *252*, 397.

(12) Blake, T. D.; Shikhmurzaev, Y. D. Dynamic Wetting by Liquids of Different Viscosity. *J. Colloid Interface Sci.* **2002**, *253*, 196.

(13) Chi, M. P.; Anh, N. V.; Evans, G. M. Assessment of Hydrodynamic and Molecular-Kinetic Models Applied to the Motion of the Dewetting Contact Line between a Small Bubble and a Solid Surface. *Langmuir* **2003**, *19*, 6796.

(14) Christov, N. C.; Ganchev, D. N.; Vassileva, N. D.; Denkov, N. D.; Danov, K. D.; Kralchevsky, P. A. Capillary Mechanisms in Membrane Emulsification: Oil-in-Water Emulsions Stabilized by Tween 20 and Milk Proteins. *Colloids Surf. A* **2002**, *209*, 83.

(15) Kao, R. L.; Wasan, D. T.; Nikolov, A. D.; Edwards, D. A. Mechanisms of Oil Removal from a Solid Surface in the Presence of Anionic Micellar Solutions. *Colloids Surf.* **1988/89**, *34*, 389.

(16) Kolev, V. L.; Kochijashky, I. I.; Danov, K. D.; Kralchevsky, P. A.; Broze, G.; Mehreteab, A. Spontaneous Detachment of Oil Drops from Solid Surfaces: Governing Factors. *J. Colloid Interface Sci.* **2003**, *257*, 357.

(17) Adamson, A. W.; Gast, A. P. *Physical Chemistry of Surfaces*, 6th ed.; Wiley: New York, 1997; Chapter IV.

(18) Nikolov, A. D.; Wasan, D. T.; Chengara, A.; Koczo, K.; Policello, G. A.; Kolossvary, I. Superspreading Driven by Marangoni Flow. *Adv. Colloid Interface Sci.* **2002**, *96*, 325.

(19) Christian, S. D.; Scamehorn, J. F. *Solubilization in Surfactant Aggregates*; Marcel Dekker: New York, 1995.

(20) Cutler, W. G., Kissa, E., Eds. *Detergency: Theory and Technology*; Marcel Dekker: New York, 1987.

(21) Dillan, K. W.; Goddard, E. D.; McKenzie, D. A. Oily Soil Removal from a Polyester Substrate by Aqueous Nonionic Surfactant Systems. *J. Am. Oil Chem. Soc.* **1979**, *56*, 59.

(22) Mahé, M.; Vignes-Adler, M.; Rosseau, A.; Jacquin, C. G.; Adler, P. M. Adhesion of Droplets on a Solid Wall and Detachment by a Shear Flow. I. Pure System. *J. Colloid Interface Sci*. **1988**, *126*, 314.

(23) Carroll, B. Physical Aspects of Detergency. *Colloids Surf. A* **1993**, *74*, 131.

(24) Miller, C. A.; Raney, K. H. Solubilization−emulsification mechanisms of detergency. *Colloids Surf. A* **1993**, *74*, 169.

(25) Thompson, L. The Role of Oil Detachment Mechanisms in Determining Optimum Detergency Conditions. *J. Colloid Interface Sci*. **1994**, *163*, 61.

(26) Kralchevsky, P. A.; Nagayama, K. *Particles at Fluid Interfaces and Membranes*; Elsevier: Amsterdam, The Netherlands, 2001; Chapter 6, p 268.

(27) von Bahr, M.; Tiberg, F.; Zhmud, B. V. Spreading Dynamics of Surfactant Solutions. *Langmuir* **1999**, *15*, 7069.

(28) Eriksson, J.; Tiberg, F.; Zhmud, B. V. Wetting Effects due to Surfactant Carryover through the Three-Phase Contact Line. *Langmuir* **2001**, *17*, 7274.

(29) Rams, E. The Spreading of Surfactant-Laden Liquids with Surfactant Transfer through the Contact Line. *J. Fluid Mech.* **2001**, *440*, 205.

(30) Davis, A. N.; Morton, S. A., III; Counce, R. M.; DePaoli, D. W.; Hu, M. Z.-C. Ionic Strength Effects on Hexadecane Contact Angles on a Gold-Coated Glass Surface in Ionic Surfactant Solutions. *Colloids Surf. A* **2003**, *221*, 69.

(31) Kumar, N.; Varanasi, K.; Tilton, R. D.; Garoff, S. Surfactant Self-Assembly ahead of the Contact Line on a Hydrophobic Surface and Its Implications for Wetting. *Langmuir* **2003**, *19*, 5366.

(32) Chatterjee, J. Critical Eotvos Numbers for Buoyancy-Induced Oil Drop Detachment Based on Shape Analysis. *Adv. Colloid Interface Sci*. **2002**, *98*, 265.

(33) Chatterjee, J. Shape Analysis Based Critical Eotvos Numbers for Buoyancy-Induced Partial Detachment of Oil Drops from Hydrophilic Surfaces. *Adv. Colloid Interface Sci*. **2002**, *99*, 163.

(34) Attard, P. Thermodynamic Analysis of Bridging Bubbles and a Quantitative Comparison with the Measured Hydrophobic Attraction. *Langmuir* **2000**, *16*, 4455.

(35) de Ruijter, M. J.; Blake, T. D.; de Coninck, J. Dynamic Wetting Studied by Molecular Modeling Simulations of Droplet Spreading. *Langmuir* **1999**, *15*, 7836.

(36) de Ruijter, M. J.; de Coninck, J.; Oshanin, G. Droplet Spreading: Partial Wetting Regime Revisited. *Langmuir* **1999**, *15*, 2209.

(37) Semal, S.; Voué, M.; de Coninck, J. Dynamics of Spontaneous Spreading on Energetically Adjustable Surfaces in a Partial Wetting Regime. *Langmuir* **1999**, *15*, 7848.

(38) de Ruijter, M. J.; Charlot, M.; Voué, M.; de Coninck, J. Experimental Evidence for Several Time Scales in Drop Spreading. *Langmuir* **2000**, *16*, 2363.

(39) Decamps, C.; de Coninck, J. Dynamics of Spontaneous Spreading under Electrowetting Conditions. *Langmuir* **2000**, *16*, 10150.

(40) Seveno, D.; Ledauphin, V.; Matric, G.; Voué, M.; de Coninck, J. Spreading Drop Dynamics on Porous Surfaces. *Langmuir* **2002**, *18*, 7496.

(41) Seveno, D.; de Coninck, J. Possibility of Different Time Scales in the Capillary Rise around a Fiber. *Langmuir* **2004**, *20*, 737.

(42) von Bahr, M.; Tiberg, F.; Zhmud, B. Oscillations of Sessile Drops of Surfactant Solutions on Solid Substrates with Differing Hydrophobicity. *Langmuir* **2003**, *19*, 10109.

(43) Todorov, P. D.; Marinov, G. S.; Kralchevsky, P. A.; Denkov, N. D.; Broze, G.; Mehreteab, A. Kinetics of Triglyceride Solubilization by Micellar Solutions of Nonionic Surfactant and Triblock Copolymer: 3. Experiments with Single Drops. *Langmuir* **2002**, *18*, 7896.

(44) Rusanov, A. I.; Prokhorov, V. A. *Interfacial Tensiometry*; Elsevier: Amsterdam, The Netherlands, 1996.

(45) Gibbs, J. W. *The Scientific Papers of J. W. Gibbs*; Dover: New York, 1961; Vol. 1.

(46) Tadros, Th. F.; Lyklema, J. Adsorption of Potential-Determining Ions at the Silica-Aqueous Electrolyte Interface and the Role of Some Cations. *J. Electroanal. Chem.* **1968**, *17*, 267.

(47) Iler, R. K. *The Chemistry of Silica: Solubility, Polymerization, Colloid and Surface Properties and Biochemistry*; Wiley: New York, 1979.

(48) Hunter, R. *Foundation of Colloid Science*; Clarendon Press: Oxford, U.K., 1987.

(49) Doremus, R. H. *Glass Science*, 2nd ed.; Wiley: New York, 1994.

(50) Vigil, G.; Xu, Z.; Steinberg, S.; Israelachvili, J. N. Interactions of Silica Surfaces. *J. Colloid Interface Sci.* **1994**, *165*, 367.

(51) Trens, P.; Denoyel, R.; Guilloteau, E. Evolution of Surface Composition, Porosity, and Surface Area of Glass Fibers in a Moist Atmosphere. *Langmuir* **1996**, *12*, 1245.

(52) Yaminsky, V. V.; Ninham, B. W.; Pashley, R. M. Interaction between Surfaces of Fused Silica in Water. Evidence of Cold Fusion and Effects of Cold Plasma Treatment. *Langmuir* **1998**, *14*, 3223.

(53) van Duijvenbode, R. C.; Koper, G. J. M.; Böhmer, M. R. Adsorption of Poly(propylene imine) Dendrimers on Glass. An Interplay between Surface and Particle Properties. *Langmuir* **2000**, *16*, 7713.

(54) Adler, J. J.; Rabinovich, Y. I.; Moudgil, B. M. Origins of the Non-DLVO Force between Glass Surfaces in Aqueous Solution. *J. Colloid Interface Sci.* **2001**, *237*, 249.

(55) Landau, L. D.; Lifshitz, E. M. *Fluid Mechanics*; Pergamon Press: Oxford, U.K., 1984.

(56) Korn, G. A.; Korn, T. M. *Mathematical Handbook*; McGraw-Hill: New York, 1968.

(57) Press, W. H.; Teukolsky, S. A.; Vetterling, W. T.; Flannery, B. P. *Numerical Recipes in Fortran. The Art of Scientific Computing*, 2nd ed.; Cambridge University Press: Cambridge, U.K., 1992; p 678.

(58) Pletnev, M. Y. in *Surfactants: Chemistry, Interfacial Properties, Applications*; Fainerman, V. B., Möbius, D., Miller, R., Eds.; Elsevier: Amsterdam, The Netherlands, 2001; Chapter 1.

(59) Kralchevsky, P. A.; Danov, K. D.; Broze, G.; Mehreteab, A. Thermodynamics of Ionic Surfactant Adsorption with Account for the Counterion Binding: Effect of Salts of Various Valency. *Langmuir* **1999**, *15*, 2351.

(60) Dimov, N. K.; Ahmed, E. H.; Alargova, R. G.; Kralchevsky, P. A.; Durbut, P.; Broze, G.; Mehreteab, A. Deposition of Oil Drops on a Glass Substrate in Relation to the Process of Washing. *J. Colloid Interface Sci.* **2000**, *224*, 116.

Received for review August 27, 2004
Revised manuscript received October 22, 2004
Accepted October 25, 2004

IE049211T